International Journal of Science and Research (IJSR)
ISSN: 2319-7064
Impact Factor 2024: 7.101

Theoretical Investigation of the Surface Properties of the Superheavy Nuclei $Z = 126$

Santosh Kumar[1]* and S. K. Singh[1]
[1]*Department of Physics, Patliputra University, Patna-800020, India*

We have thoroughly investigated the surface characteristics, including symmetric energy, neutron pressure, and symmetry energy curvature coefficient, from the proton to neutron drip-lines for a hypothetical super heavy nucleus $Z = 126$. We use relativistic mean field model with well known force parameter like NL3 and NLB in our calculations for finite nuclei. The relativistic mean-field densities use as input in the Coherent Density Fluctuation Model (CDFM) to calculate the surface properties of the system. Before determining the surface characteristics of the finite nuclei, the expected bulk properties like binding energy, charge radius and neutron skin thickness are calculated.

Key words: Relativistic Mean Field; Charge Distribution; symmetry energy; Neutron Pressure; symmetry energy curvature coefficients.

I. INTRODUCTION

The main interest of the current time is to constraint the observable range with the help of theoretical and experimental outcomes. Due to advance computational and experimental facilities like HIC, FRIB, PREX, these correlation can be done very precisely. The surface properties of the finite nuclei and nuclear matter is very fundamental to control the many structural and dynamics of the system. The surface properties of finite nuclei like symmetry energy, neutron skin thickness, etc are always playing an important role in nuclear matter and astrophysics properties. The symmetric energy characterizes the equation of state (EoS) for nuclear matter in connection with isospin asymmetry. The symmetry energy is also established the range for the neutron star properties like mass and radius [1]. The surface characteristics inherently regulate the neutron star (NS) merger conditions, gravitational waves (GW), and additional factors. The correlation between symmetric energy of nuclear matter and the thickness of the neutron skin in finite nuclei [2] make the possible to investigate the structure of neutron stars by understanding the equation of state (EoS). The symmetry energy has attracted interest because of astrophysical observations and the presence of advance unique beams facilities in laboratories [3]. The study of symmetry energy is also important observable to identify magic nuclei [3, 4].

The non-relativistic Skyrme-Hartree-Fock method forecasts nuclear magicity for $Z > 114$, suggests double magicity at $Z = 126$ and $N = 184$, and shows enhanced stability at $N = 162$ due to deformed shell effects [5]. In another work, the author Manjunatha [6] examined the alpha decay characteristics of superheavy nuclei Z=126 and forecasted that the cores 126^{307}, 126^{318} 126^{319}, 126^{320} were discovered to possess extended alpha decay half-lives and therefore might be detectable if produced in a laboratory setting. The potential for a proton magic number at $Z = 126$ has been a topic of discussion since 1955 [7]. After the nuclear shell model was developed, the possibility of stable nuclides at $Z = 126$ was investigated; the results were controversial [8–11]. The DRHBc computations with PC-PK1 are employed to determine the even-even $Z = 126$ isotopes. To explore possible nuclear magic, the changes in quadrupole deformation and the energies of neutron and proton pairing are analyzed. There exist circular forms and Proton pairing energy remains present in $Z = 126$ isotopes, while neutron pairing energy vanishes at $N = 258$ and 350, signifying these as neutron magic numbers. No significant gap is observed in the single-proton spectra at $Z = 126$, yet there are considerable gaps at $Z = 120 and 138$. Consequently, $Z = 120 and 138$ are suggested as possible proton magic numbers, while $Z = 126$ is not validated [12]. The considered system ($Z = 126$) is viewed as a magic number since contemporary nuclear shell models forecast a significant proton shell gap at $Z = 126$, resulting from intense spin–orbit coupling and relativistic influences in superheavy nuclei.

In this study, we investigate the effective surface properties in isotopic series of $Z = 126$ nuclei by assessing the bulk characteristics and densities of the nuclei using the relativistic extended Thomas Fermi model (RETF). The RETF approximation gives more accurate results for bigger mass system as compare to ligher nuclei. We have calculated the bulk properties and density profile for the isotopic chain of considered nuclei $Z = 126$. We use coherent density functional model to calculate the further surface properties like symmetry energy, neutron pressure and curvature parameter. The CDFM offers a benefit compared to other methods as it tackles (i) the variation in the nuclear density distribution by employing the weight function $|f(x)|^2$ and (ii) the momentum distributions through the mixed density matrix, namely the Wigner distribution function [3, 4, 13].

The organization of the paper is outlined as follows: Section II addresses the relativistic mean-field model and describes the process of adjusting the energy density functional to a mathematical form in coordinate space by employing the Bruckner method [14]. A short overview of the CDFM is also included. The outcomes of our calcula-

* sankm036@gmail.com

tions are addressed in Section III. Section III E provides a summary along with final observations.

II. THEORETICAL FORMALISM

A. Effective field theory model

The Virial theorem is obtained from the relativistic mean-field Hamiltonian within the extended relativistic Thomas-Fermi method (RETF) in the scaling framework [15–17, 19–23].

To ensure completeness, we have concisely reviewed several key formulas that are crucial for the calculations conducted σ. The correlations among numerous particles stemming from the nonlinear features of meson self-interaction were examined utilizing the nonlinear Lagrangian introduced by Boguta and Bodmer [24]

The relativistic mean field nucleon-meson interacting system's Hamiltonian is expressed as [15–18, 25, 26]:

$$\begin{aligned}\mathcal{H} &= \sum_i \varphi_i^\dagger \Big[-i\vec{\alpha}\cdot\vec{\nabla} + \beta m^* + g_v V + \frac{1}{2} g_\rho R\tau_3 + \frac{1}{2} e\mathcal{A}(1+\tau_3)\Big]\varphi_i + \frac{1}{2}\left[(\vec{\nabla}\phi)^2 + m_s^2\phi^2\right] \\ &+ \frac{1}{3}b\phi^3 + \frac{1}{4}c\phi^4 - \frac{1}{2}\left[(\vec{\nabla}V)^2 + m_v^2 V^2\right] - \frac{1}{2}\left[(\vec{\nabla}R)^2 + m_\rho^2 R^2\right] - \frac{1}{2}\left(\vec{\nabla}\mathcal{A}\right)^2 \end{aligned} \quad (1)$$

The related fields are ϕ, V, and A for the σ, ω, $\rho-$mesons, and photon.

The τ_3 is the third component of the iso-spin for the $\rho-$meson. Due to its fluctuations in the mesonic medium, the nucleon's actual mass m seems to be obscured, resulting in its effective mass $m^* = m - g_s\phi$. The masses of the σ-, ω- and ρ- mesons are denoted as m_s, m_v, and m_ρ, respectively. The coupling constants g_s, g_v, g_ρ, and $e^2/4\pi$=1/137 show how nucleons interact with σ, ω, ρ-mesons, and photons. In the nonlinear $\sigma-\omega$ model, the self-limiting factors of the $\sigma-$meson field are b and c. Variational methods can be used to derive the equations of motion for meson and nucleon fields.

The density's Hamiltonian in the semiclassical approximation has the following expression:

$$\mathcal{H} = \mathcal{E} + g_v V\rho + g_\rho R\rho_3 + e\mathcal{A}\rho_p + \mathcal{H}_f, \quad (2)$$

with,

$$\mathcal{E} = \sum_i \varphi_i^\dagger \Big[-i\vec{\alpha}\cdot\vec{\nabla} + \beta m^*\Big]\varphi_i. \quad (3)$$

In this case, the free part of the Hamiltonian is represented by $\mathcal{H}_f$, and the total density ρ is the sum of the distribution densities of protons (rho_p) and neutrons (rho_n). The center of mass kinetic energy correction factor (cm) is determined by the harmonic oscillator equation $E_{c.m.} = \frac{3}{4}(41A^{-1/3})$. Here A is the mass number of the atomic nucleus. The root mean square charge radius (R_{ch}), proton radius (R_p), neutron radius (R_n), and matter radius (R_{rms}) are as follows:

$$< R_p^2 >= \frac{1}{Z}\int \rho_p(r_\perp, z) r_p^2 d\tau_p, \quad (4)$$

$$< R_n^2 >= \frac{1}{N}\int \rho_n(r_\perp, z) r_n^2 d\tau_n, \quad (5)$$

$$R_{ch} = \sqrt{R_p^2 + 0.64}, \quad (6)$$

$$< R_{rms}^2 >= \frac{1}{A}\int \rho(r_\perp, z) r^2 d\tau. \quad (7)$$

In this context, all terms retain their standard meanings. The overall binding energy of the system and various observables can be derived from their conventional relationships [27–29]

B. Coherent density Fluctuation Model

The CDFM was developed and suggested in References [30, 31]. The one-body density matrix ρ (**r, r**$'$) of a nucleus can be represented in the CDFM as a coherent superposition of an infinite number of one-body density matrices ρ_x (**r**, **r**$'$) corresponding to spherical particles of nuclear matter referred to as *Fluctons* [3, 4, 30]:

$$\rho_x(\mathbf{r}) = \rho_0(x)\Theta(x - |\mathbf{r}|), \quad (8)$$

with $\rho_o(x) = \frac{3A}{4\pi x^3}$. The spherical radius of the nucleus in a uniformly distributed spherical Fermi gas is the generator coordinate x. In a finite nuclear system, the one-body density matrix can be represented as [3, 4, 13, 30],

$$\rho(\mathbf{r}, \mathbf{r}') = \int_0^\infty dx |f(x)|^2 \rho_x(\mathbf{r}, \mathbf{r}'), \tag{9}$$

where, $|f(x)|^2$ is the weight function (Eq. (13)). The term $\rho_x(\mathbf{r}, \mathbf{r}')$ is the coherent superposition of the one body density matrix and defined as,

$$\rho_x(\mathbf{r}, \mathbf{r}') = 3\rho_0(x) \frac{J_1\left(k_f(x)|\mathbf{r} - \mathbf{r}'|\right)}{\left(k_f(x)|\mathbf{r} - \mathbf{r}'|\right)} \times \Theta\left(x - \frac{|\mathbf{r} + \mathbf{r}'|}{2}\right) \tag{10}$$

The first-order spherical Bessel function is denoted as J_1 here. The Fermi momentum of the nucleons in the Fluctons with radius x can be expressed as $k_f(x)=(3\pi^2/2\rho_0(x))^{1/3} = \gamma/x$, where $\gamma=(9\pi A/8)^{1/3} \approx 1.52A^{1/3}$.

The Wigner distribution function of the one body density matrices in Eq. (10) is,

$$W(\mathbf{r}, \mathbf{k}) = \int_0^\infty dx |f(x)|^2 W_x(\mathbf{r}, \mathbf{k}). \tag{11}$$

Here, $W_x(\mathbf{r}, \mathbf{k}) = \frac{4}{8\pi^3}\Theta(x - |\mathbf{r}|)\Theta(k_F(x) - |\mathbf{k}|)$. Similarly, the density ρ (r) within CDFM can express in terms of the same weight function as,

$$\rho(r) = \int d\mathbf{k} W(\mathbf{r}, \mathbf{k}) = \int_0^\infty dx |f(x)|^2 \frac{3A}{4\pi x^3}\Theta(x - |\mathbf{r}|) \tag{12}$$

and it is normalized to the nucleon numbers of the nucleus, $\int \rho(\mathbf{r}) d\mathbf{r} = A$. By taking the δ-function approximation to the Hill-Wheeler integral equation, we can obtain the differential equation for the weight function in the generator coordinate [4, 30]. The weight function for a given density distribution ρ (r) can be expressed as,

$$|f(x)|^2 = -\left(\frac{1}{\rho_0(x)} \frac{d\rho(r)}{dr}\right)_{r=x}, \tag{13}$$

with $\int_0^\infty dx |f(x)|^2 = 1$. For a detailed analytical derivation, one can follows Refs. [4, 32, 33]. The symmetry energy, neutron pressure, and symmetry energy curvature for a finite nucleus are defined by evaluating the corresponding values for infinite nuclear matter in the CDFM. The characteristics of finite nuclei can be derived from those of nuclear matter through the CDFM. The curvature ΔK, pressure P, and effective symmetry energy S of a nucleus can be represented using the CDFM method as [3, 4, 13, 32–34]

$$S = \int_0^\infty dx |f(x)|^2 S_0^{NM}(\rho(x)), \tag{14}$$

$$P = \int_0^\infty dx |f(x)|^2 P_0^{NM}(\rho(x)), \tag{15}$$

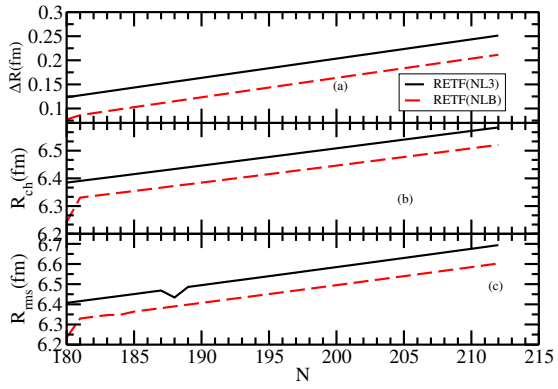

FIG. 1. The neutron skin thickness, charge radius R_{ch}, and matter radius R_{rms} as functions of neutron number for $Z = 126$ isotopes are determined using relativistic mean field theory with Extended Thomas Fermi (RETF-NL3) [17] (solid black line) and compared to the RETF-NLB [35] (dashed red line) force parameters for particular nuclei

.

$$\Delta K = \int_0^\infty dx |f(x)|^2 \Delta K_0^{NM}(\rho(x)). \tag{16}$$

For describing $S_0^{NM}(x)$, $P_0^{NM}(x)$, and $\Delta K_0^{NM}(x)$ we direct readers to the paper [14] for the complete details.

III. RESULTS AND DISCUSSIONS

A. Charge radius, matter radius distributions and neutron skin thickness

In our examination, we focused on the distribution of nucleons. In this section, we present the findings regarding the radius of the analyzed system within its isotopic series. The Figure1(a–c) illustrates the neutron skin thickness (a), charge radius (b), and root-mean-square (c) radius as a function of neutron number (N) for isotopes with atomic number $Z = 126$, computed using the relativistic mean-field (RMF) approach with the NL3 and NLB force parameters.

The thickness of the neutron skin $\Delta R = R_n - R_p$ is shown in Fig. 1 (a). A consistent rise in ΔR takes place with the increase in neutron number for both RMF interactions. This behavior indicates a increasing imbalance between protons and neutrons, resulting in a broader distribution of neutron density at the surface of the nucleus. By adding extra neutrons, these particles predominantly occupy higher energy orbitals that extend further radially, thereby enlarging the neutron skin. Although both parameterizations exhibit similar trends, slight quantitative variations are apparent, indicating a moderate sensitivity of ΔR to the isovector component of the RMF interaction. The figure 1 (b) shows the variations in the

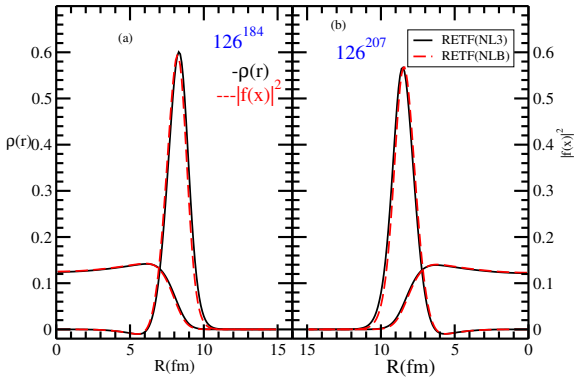

FIG. 2. The density and weight function obtained as a function of neutron number for $Z = 126$ isotopes are computed using relativistic mean field theory with Extended Thomas-Fermi (RETF-NL3) [17] (solid black line) and compare to RETF-NLB [35](dashed red line) force parameters for selected nuclei

.

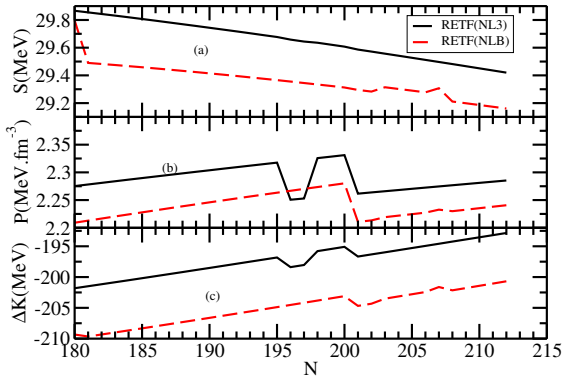

FIG. 3. The (a) symmetry energy (S), (b) neutron pressure (P), and (c) symmetry energy curvature coefficients ΔK as a function of neutron number for $Z = 126$ isotopes are computed using relativistic mean field theory with Extended Thomas-Fermi (RETF-NL3) [17] (solid black line) and compared to RETF-NLB [35] (dashed red line) force parameters for specific nuclei

.

charge radius involving neutron number. The charge radius steadily increases as more neutrons are incorporated into the nucleus. This rise results from the connection between neutron and proton densities via the nuclear interaction, leading to a minor outward displacement of the proton distribution. The gradual development of R_{ch} indicates that there are no sudden structural changes in the examined isotopic chain. The strong correlation between NL3 and NLB outcomes suggests that the charge radius is quite unaffected by the selection of RMF parameter set. The figure 1 (c), In both types of interactions, the rms radius steadily grows with the neutron numbers. The increase in the rms radius is directly linked to the overall growth in nuclear size with rising mass numbers, as it reflects the collective spatial distributions of protons and neutrons. Across the examined neutron range, the derived rms radii display a uniform trend, indicating a continual structural change within the nucleus in both force parameters.

B. Densities and Weight Function

We are discussing the mainly surface properties in this section. We use the density from the RMF model within RETF approximation in CDFM to calculate the surface properties of the considered nuclei. The results are given in figure 2, which displays the radial density distributions and weight function as a function of neutron count for $Z = 126$, computed using the relativistic mean-field approach with $NL3$ and NLB force parameter sets. The results for the density and weight function for $Z = 126$ are shown for the isotopes 126^{184} and 126^{207}, which is located within the area of predicted "island of stability" for super-heavy elements. The panel in Figure 2, illustrates the weight functions for the nuclei 126^{184} and 126^{207} as examples. The illustration indicates that the weight function represents variations in the density profile. Both interactions predict a comparable qualitative density profile, including the center depletion and the enlarged surface region, according to a comparison of the NL3 and NLB parameterizations. Although there are slight quantitative variations in the surface diffuseness and the depth of the central depression, overall agreement indicates that the bubble-like density distribution is a reliable and model-independent feature for nuclei with Z=126. The microscopic basis of this behavior is explained in the right pannel of the Fig. 2, which shows the squared radial wave function. This radial localization means that nucleons in these orbitals steer clear of the nucleus central area, thus directly contributing to the observed reduction in central density. The stability, decay characteristics, and reaction dynamics of super-heavy nuclei near the anticipated island of stability may be significantly impacted by these characteristics.

C. Effective surface properties of the super heavy nuclei

The figure 3 displays the progression of the symmetry energy(S), neutron Pressure(P), along with the symmetry energy curvature coefficient ΔK as a function of neutron count for isotopes with a specific atomic number $Z = 126$, computed using the relativistic mean-field approach with $NL3$ and NLB force parameter sets.

The symmetry energy(S) display in figure 3 (a),

demonstrates a steady and almost linear rise with neutron number across the range $N = 180$–212. For both the parameter force examined, the strength of Symmetry energy(S) remains near 30 MeV, suggesting that the primary isovector characteristics of nuclear matter are only slightly altered with higher neutron excess. However, a distinct model dependence is noted in the slope of the symmetry energy, indicating variations in the density dependence of the isovector interaction. The rise of Symmetry energy (S) with neutron number indicates a higher energetic expense linked to sustaining substantial neutron–proton asymmetry in superheavy nuclei.

The figure3 (b) illustrates with the associated neutron pressure (P) as a function of the number of neutrons. An uninterrupted rise in neutron pressure (P) is monitored for both the NL3 and NLB RMF interaction. This behavior is directly tied to the rising slope of the symmetry energy and signifies an increasing repulsive influence from the isovector channel as more neutrons are included. Parameter sets defined by a more rigid symmetry energy forecast consistently greater neutron pressures. The rise in neutron pressure indicates a forceful ejection of surplus neutrons, likely to increase neutron skin thickness and affect the spatial extent and stability of neutron-rich superheavy nuclei.

The figure3 (c) depicts the variation in the curvature coefficients of symmetry energy ΔK as a function of neutron count. ΔK reliant on neutron count N for nuclei having $Z = 126$, established with the RMF model using NL3 and NLB force parameters, reveals a typical configuration in RMF(RETF) calculations for $N = 195 - 202$. In RMF(NLB) calculations at $N = 201$, enhanced shell effects suggest possible sub-shell closures and increased stability for these neutron numbers

D. Correlation of neutron skin-thickness with the surface properties

In this section we try to explain the correlation properties between neutron skin thickness and surface properties of selected isotopes of the superheavy nuclei $Z = 126$. The figures 4(a)–(c) shows importance of symmetry energy parameters are influenced by the thickness of the neutron skin $\Delta R = R_n$-R_p as derived in the relativistic mean-field (RMF) approach employing NL3 and NLB force parameter sets.

The figure 4 (a) illustrates the changes in symmetry energy(S) at saturation density, depending on the neutron skin thickness. A distinct and almost linear rise of Symmetry energy (S) with rising ΔR is noted for both $NL3$ and NLB RMF parameterizations examined. This consistent pattern suggests that nuclear models forecasting a thicker neutron skin correlate with higher symmetry energy values. Despite the existence of quantitative variations both the NL3 and NLB force parameter sets, the positive correlation is consistently strong, indicating that neutron skin thickness serves as a critical observable for

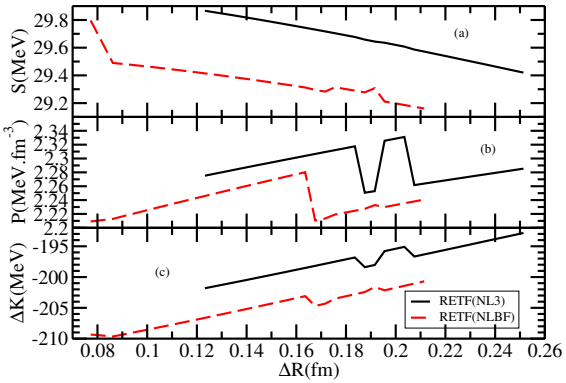

FIG. 4. The (a) symmetry energy (S), (b) neutron pressure (P), and (c) symmetry energy curvature coefficients ΔK as a function of neutron skin thickness (ΔR) for $Z = 126$ isotopes, calculated with relativistic mean field theory through Extended Thomas-Fermi (RETF) [17] (black solid line) and compared with Non-linear Boson (NLB) [35] (red dashed line) force parameters for certain selected nuclei

.

limiting the size of the symmetry energy. Figure 4 (b) shows the neutron pressure(P) in neutron rich matter as a function of the thickness of the neutron skin. The pressure demonstrates a significant consistent rise with growing ΔR. Relative to the symmetry energy itself, the connection between neutron pressure and neutron skin thickness is clearer. This behavior indicates that models exhibiting greater neutron pressure push neutrons more outward in finite nuclei, leading to a thicker neutron skin thickness. The figure 4 emphasizes neutron skin thickness as a direct indicator of the pressure in neutron-rich matter close to saturation density. The figure 4 (c) illustrates the relationship of symmetry energy curvature coefficient ΔK with ΔR. It is changes in a systematic manner with ΔR, become increasingly less negative as the neutron skin expands. This trend indicates that neutron skin thickness is influenced not only by the magnitude and pressure linked to symmetry energy but also by its higher order dependence on density.

E. summary and conclusions

The collective behavior of neutron skin thickness, charge radius, and rms radius offers a thorough overview of the size development in neutron-rich superheavy nuclei with $Z = 126$. The noticeable rise in neutron skin thickness underscores the significant influence of surplus neutrons on the nuclear surface formation, whereas the slow growth of charge and rms radii illustrates the reaction of the proton distribution and the complete nuclear system.

These findings highlight the significance of isospin ef-

fects in superheavy nuclei and offer valuable limitations on RMF parameterizations in the highly neutron-rich domain.

[1] J. M. Lattimer et al., 2007, "Neutron Star Observations: Prognosis for Equation of State Constraints", Phys. Rept., (442),109.
[2] Bao-An Li et al., 2009, "Towards Understanding Astrophysical Effects of Nuclear Symmetry Energy", Eur.Phys. J. A, (55), 117.
[3] M. K. Gaidarov et al., 2011, "Surface properties of neutron-rich exotic nuclei: A source for studying the nuclear symmetry energy", Phys. Rev. C, (84), 034316.
[4] M. Bhuyan et al., 2018, "Surface properties of neutron-rich exotic nuclei within the relativistic mean-field formalism", Phys. Rev. C, (97), 024322.
[5] S Cwiok et al., 1996, "Shell structure of the superheavy elements", Nucl. Phys. A, (611) 211.
[6] H.C. Manjunatha et al., 2016, "Alpha decay properties of superheavy nuclei $Z = 126$", Nuclear Physics A ,(Volume 945), Pages 42-57.
[7] J. A Wheeler et al., 1955, "Nuclear fission and nuclear stability. In Niels Bohr and the Development of Physics: Essays Dedicated to Niels Bohr on the Occasion of His Seventieth Birthday", McGraw-Hill: New York, NY, USA, p. 163.
[8] F.G Werner et al., 1958, "Superheavy Nuclei." Phys. Rev., (109), 126–144.
[9] W.D Myers et al.,1966 "Nuclear masses and deformations", Nucl. Phys. ,(81), 1–60.
[10] P. J. Siemens et al,. 1967, "Shape of Heavy Nuclei", Phys. Rev. Lett. (18), 704.
[11] S. Cwiok et al., 1996, "Shell structure of the superheavy elements", ´ Nucl. Phys. A 611, 211.
[12] Cong Pan Xin-Hui Wu, 2025, "Examination of Possible Proton Magic Number Z = 126 with the Deformed Relativistic Hartree-Bogoliubov Theory in Continuum", MDPI, Particles ,(8), 2.
[13] M. K. Gaidarov et al., 2012,Symmetry energy of deformed neutron-rich nuclei
Phys. Rev. C 85, 064319.
[14] Abdul Quddus et al., 2020, "Effective surface properties of light, heavy, and superheavy nuclei" Journal of Physics G ,(Volume 47) ,4 ,045105.
[15] S. K. Patra et al., (2001), "Scaling in relativistic Thomas–Fermi approach for nuclei", Physics Letters B (523), 67-72.
[16] S. K. Patra et al., 2002, "Nuclear surface properties in relativistic effective field theory", Nucl. Phys. A ,(703), 240.
[17] Chaoyuan Zhu et al., 1991, "A study of the giant monopole state within the relativistic Thomas-Fermi approximation", J. Phys. G, (17), L11.
[18] M. Centelles et al., 2010, "The influence of the symmetry energy on the giant monopole resonance of neutron-rich nuclei analyzed in Thomas–Fermi theory" J. Phys. G (37), 075107.
[19] M. Centelles et al, 1993, "A Semiclassical Approach to Relativistic Nuclear Mean Field Theory", Ann. Phys., NY, (221), 165.
[20] M. Centelles et al., 1992, "Relativistic investigation of nuclear surface properties", Nucl. Phys.A (537), 486.
[21] C. Speichers et al., 1998, "Density Functionals:Theory and Applications", Nucl. Phys. A (562), 569.
[22] M. Centeless et al., 1998, "Semiclassical treatment of asymmetric semi-infinite nuclear matter: surface and curvature properties in relativistic and non-relativistic models", Nucl. Phys. A, (635), 193.
[23] M. Centelles, et al., 1993, "Relativistic extended Thomas-Fermi calculations of finite nuclei with realistic nucleon-nucleon interactions", Phys. Rev. C (47), 1091.
[24] J. Boguta et al., 1997, "Relativistic calculation of nuclear matter and the nuclear surface" Nucl. Phys. A (292), 413.
[25] J. Piekarewicz et al., 2002, "Correlating the giant-monopole resonance to the nuclear-matter incompressibility", Phys. Rev. C (66), 034305.
[26] B. D. Serot et al., 1986, "The Relativistic Nuclear Many Body Problem", Adv. Nucl. Phys. (16), 1.
[27] Y. K. Gambhir, et al., 1990, "Relativistic mean field theory for finite nuclei.", Ann. Phys. (NY) (198), 132.
[28] Jeet Amrit Pattnaik, et al., (2023) "Structure and reaction studies of Z = 120 isotopes using non-relativistic and relativistic mean-field formalisms", Pramana – J. Phys., (97) 136.
[29] S. K. Patra, et. al., 1991, "Relativistic mean field study of light medium nuclei away from beta stability", Phys. Rev. C, (44), 2552.
[30] A. N. Antonov et al.,1979 "Nucleon momentum distributions and nuclear structure", Bulgarian Journal of Physics, (6), 151; A. N. Antonov et al.,1980, "A model of coherent fluctuations of nuclear density", Z. Phys. A(297), 257; A. N. Antonov et al.,1982, "Short-range correlations in finite nuclei", Z. Phys.A(304), 239; A. N. Antonov et al., 1985, "Nucleon momentum distributions in nuclei", Nuovo Cimento A (86), 23; A. N. Antonov et al.,1989, "Effects of short-range correlations on nuclear one-body density matrices", Nuovo Cimento A(102), 1701; A. N. Antonov et al.,1994, "Nucleon momentum distributions, natural orbitals, and short-range correlations in nuclei", Phys. Rev. C (50), 164.
[31] A. N. Antonov et al.,1993, "Nucleon Correlations in Nuclei", Springer-Verlag,Heidelberg, (New York in Springer listing); A. N. Antonov et al.,1988, "Nucleon Momentum and Density Distributions in Nuclei" Clarendon Press, (Oxford)
[32] A. N. Antonov et al.,1994, "Effect of nucleon correlations on natural orbitals", Phys. Rev. C(50), 164.
[33] C. Fuchs et al.,1995, "Density dependent hadron field theory", Phys. Rev. C,(52),3043.
[34] A. N. Antonov et al.,2017, "Temperature dependence of the symmetry energy and neutron skins in Ni, Sn, and Pb isotopic chains", Phys. Rev. C,(95), 024314.
[35] R.J Furnstah et al., 1987, "Systematics of light deformed nuclei in relativistic mean-field models", Physical Review C, (Vol 36) , 6.